Effect of Aspect Ratio on Wing Aerodynamic Performance

Author

Mohammad Zandsalimy

December 9, 2021

Abstract

The flow characteristics over a wing with constant cross-section are studied experimentally in the low speed wind tunnel. The wing used for the experiment is made of several sections of small spans of an Eppler 85-5 section airfoil. The behaviour of the wing is studied for three different wind velocities and by varying the angle of attack, from -8 to 32 degrees. The lift and drag forces on the wing are measured using an external balance, and these results are used for the calculation of the lift and drag coefficients. The calibration of the external load cell is carried out to reduce the systematic errors in the measurement of lift and drag. Further, the tests are carried out on the wing with different aspect ratios to study its corresponding effect on the generation of the lift and drag on the wing. The results are analysed to understand the phenomenon of the stall and to determine the optimal angle of attack for different wind velocity. The closed loop wind tunnel used to carry out these experiments is not equipped with flow visualization possibility.

Contents

List of Figures

UBC THE UNIVERSITY OF BRITISH COLUMBIA

List of Tables

THE UNIVERSITY OF BRITISH COLUMBIA

Nomenclature

α Angle of Attack

μ Dynamic Viscosity

ν Kinematic Viscosity

ρ Density

C_d Drag Coefficient per Unit Span

C_l Lift Coefficient per Unit Span

D Drag Force

g Gravity Acceleration

h Liquid Column Height

L Lift Force

P Pressure

Re Reynolds Number

s Wing Span

V_t Test Section Inlet Average Velocity

C   chord

1   Introduction

Study of the fluid flow over curved boundaries is important in various industrial applications including turbo-machinery, aircraft, boats, heat exchangers, and many more. Airfoils are examples of objects with curved boundaries used in aircraft to produce lift. Different characteristics of airfoils are presented in Fig. 1. There are three different methods of analyzing fluid flow over objects; analytical approaches, numerical, and experimental methods. Because the analytical procedures are limited in the determination of some parameters such as maximum lift coefficient, characteristics after stall, determination of zero lift angle of attack, and pitching moment, numerical and experimental methods are utilized more often. Both of these methodologies have their own limitations. However, conducting experimental studies are essential and are required for data validation. Experiments on airfoils are conducted in wind tunnels to study the fluid flow over the airfoil and resulting aerodynamic forces. In the present lab, lift and drag forces on an Eppler 85-5 airfoil with 22.7% thickness are measured. The experiments are carried out in a range of Reynolds numbers and angles of attack. The profile of the Eppler 855 airfoil with 22.7% thickness is presented in Fig. 2.
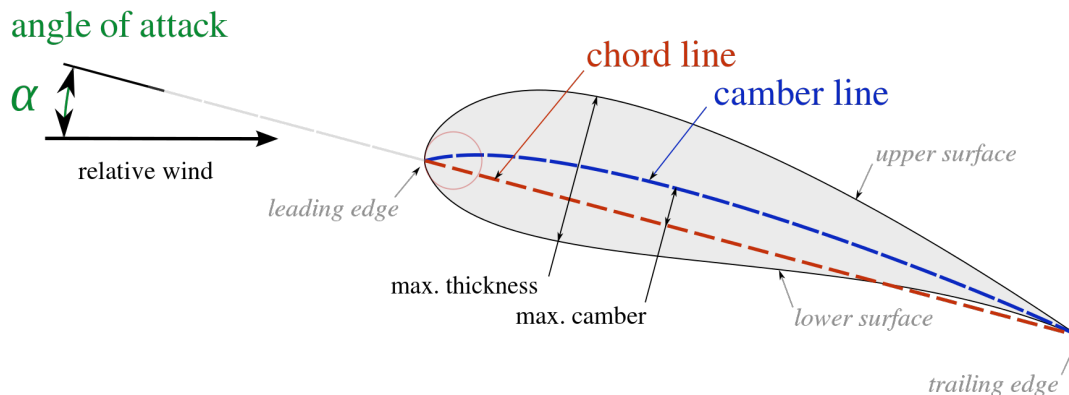
Figure 1: Typical airfoil characteristics.
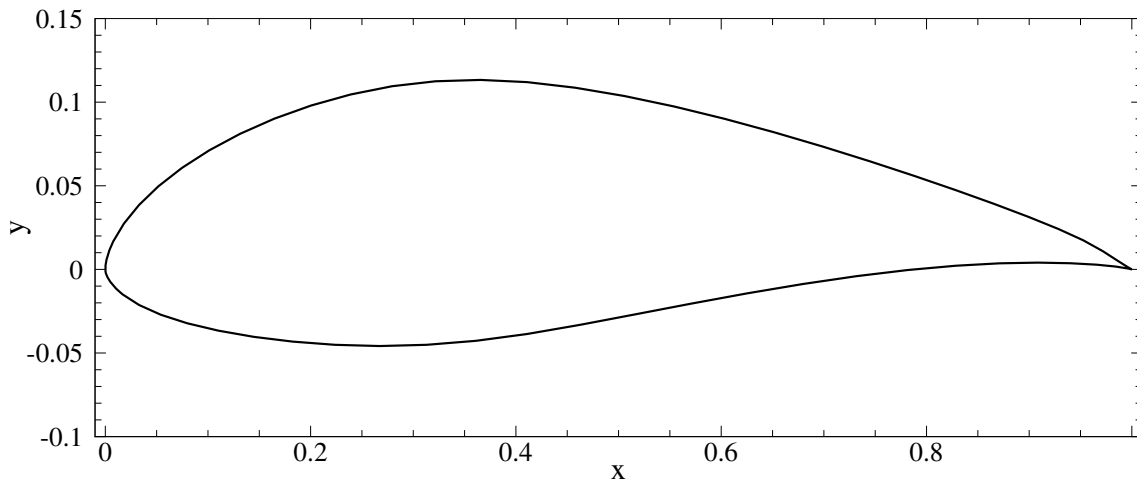
Figure 2: Eppler 855 airfoil with maximum thickness of 22.7%.

1.1   Objectives

The main objectives of this experiment are:

- Conduct experiments on a wing with an Eppler airfoil cross section

- Measure lift and drag forces using an external load cell

- Study the effect of aspect ratio on the net amount of lift and drag generated by the wing

- Analysis of uncertainty

- Reduction of data and presentation

1.2   Facility Description

The test facility includes a closed loop low speed wind tunnel located at the University of British Columbia. There are various measurement tools available for this experiment. A photo of the data acquisition PC, fan rpm controller, as well as the Betz manometer is presented in Fig. 3. The wind tunnel has a rectangular test section. For such experimental studies utilizing wind tunnels, an important test before anything else is to measure the turbulence intensity in the wind tunnel test section. Unfortunately, this is not a part of the present study and we will trust that turbulence intensity is low enough. The Betz manometer measures the pressure difference between test section entrance and outside in millimeters of water. A photo of this manometer is presented in Fig. 4. The external balance used for lift and drag measurement is presented in Fig. 5. Also, in this figure the tubes connecting pressure taps to the manometer are seen.

THE UNIVERSITY OF BRITISH COLUMBIA

Figure 3: Data acquisition, fan controller, and Betz manometer.

Figure 4: Close up of the Betz manometer.
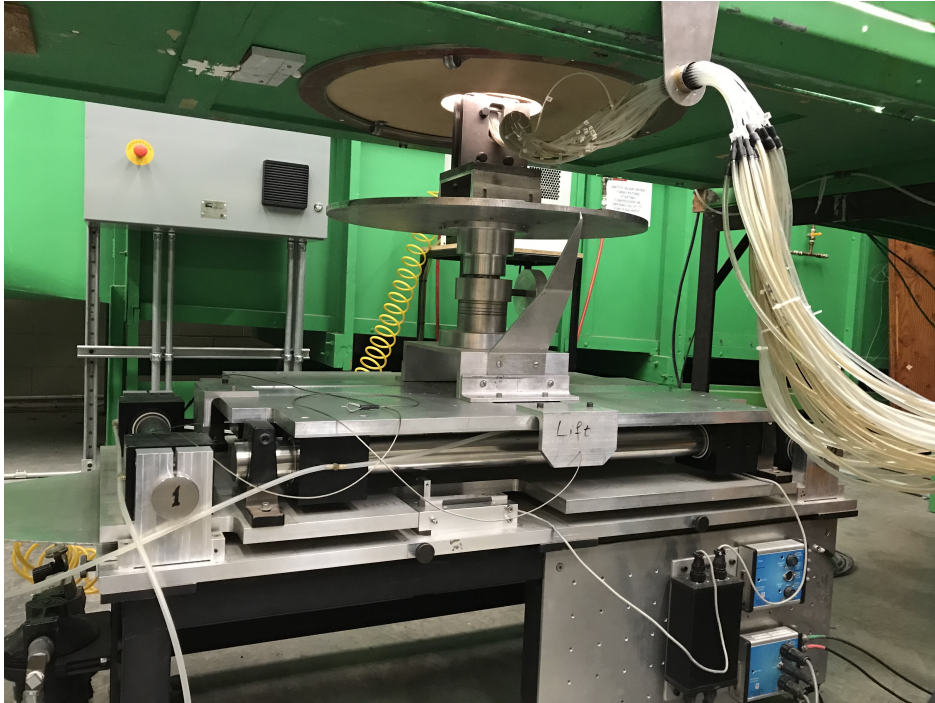
Figure 5: External load cell.

1.3   Airfoil and Wing Characteristics

Tests are carried out on an Eppler 855 airfoil with a chord of 6 inches. Initially, the wing has a span of ten 2 inch aluminum blocks plus one 2.5 inch wooden block, in total 22.5 inches. The thickness of the airfoil is 22.7% of the chord. The wing sections are held in place by two span-wise rods.

2   Theory

The drag force is the component of force on a body acting parallel to the direction of free stream. The drag coefficient C_d is the ratio of drag force to the wetted area of a wing times the dynamic head of free stream flow. If compressibility and free surface effects are neglected, drag coefficient is a function of Reynolds number only. The total drag force is the sum of the friction drag and pressure drag. Lift force acts on an immersed body normal to the relative free stream. The lift coefficient C_l is the ratio of lift force to the wetted area of a wing times the dynamic head of free stream flow. The net lift force generated by a finite wing strongly depends on the span. Smaller span usually translates into less net lift force. This is not true in the case of 3D Delta wings. The lift coefficient may be calculated from the pressure distributions on the upper and lower surfaces as well. Pitching moment is the moment acting in the plane containing the lift and the drag. It is positive when it tends to increase the angle of attack. Coefficient of pitching moment is the ratio of Pitching moment to wetted area times free stream dynamic head times chord.

3   Approach

The first step for a successful experimental testing is to calibrate the measurement tool to reduce the systematic errors as much as possible. The static calibration is carried out for the external balance. This balance should be calibrate in two directions; parallel to test section flow (drag calibration) and normal to the flow (lift calibration). A range of loads are applied to get the relation between loads and the reading of the data acquisition system. The weights applied to the balance for drag calibration and the data readings are presented in table 1. Note that the measured values of the data acquisition system have units of Newtons, however, for the sake of this lab we will assume that we don't know the units. By plotting the data in Fig. 6 we can estimate any value of reading vs. the actual force with a simple linear relation fit. This relation is found to be as Eq. 1 using Matlab software. In this equation, $D(x)$ is the actual drag force and x is the reading value. Also, the uncertainty is the maximum value of the standard deviation.

Table 1: Drag calibration data.

Mass [kg]	Weight [N]	Measured Value
0.113	1.10853	1.133
0.313	3.07053	3.090
0.513	5.03253	5.048
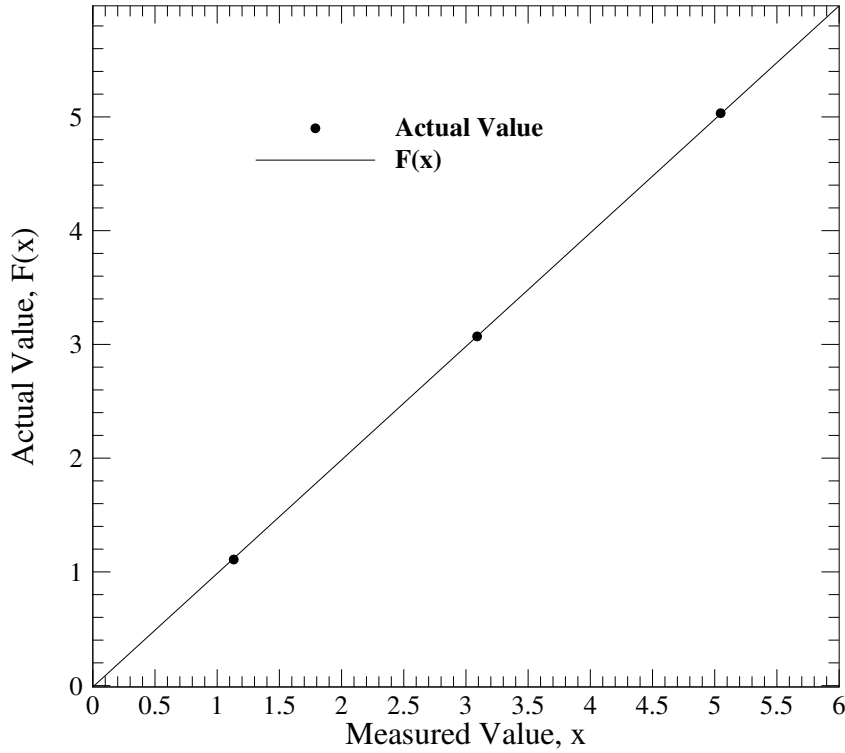
Figure 6: Drag calibration data.

$$D(x) = 0.9984x - 0.0117 \quad N \tag{1}$$

The same procedure is repeated for the lift calibration. The weights applied to the balance for lift calibration and the data readings are presented in table 2. By plotting the data in Fig. 7 we can estimate any value of reading vs. the actual force with a simple linear relation fit. This relation is found to be as Eq. 2 using Matlab software. In this equation, $L(x)$ is the actual lift force and x is the reading value. Also, the uncertainty is the maximum value of the standard deviation.

Table 2: Lift calibration data.

Mass [kg]	Weight [N]	Measured Value
0.113	1.10853	1.075
0.313	3.07053	3.007
0.513	5.03253	4.908
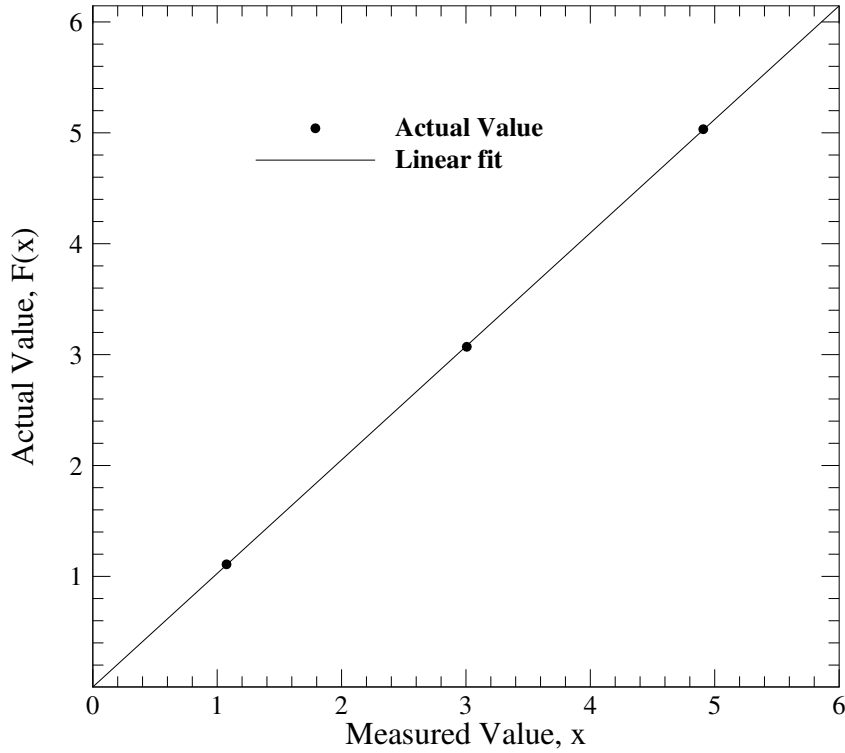
Figure 7: Lift calibration data.

$$L(x) = 1.0237x + 0.0028 \quad N \tag{2}$$

3.1 Liquid Properties

The temperature of testing area was recorded to be $20°C$. Using standard liquid property tables we can construct a useful table for the calculations of pressure and velocity. The properties of air, water, and ethyl alcohol at $20°C$ are presented in table 3.

Table 3: Liquid properties at $20°C$.

Liquid	Density (ρ) kg/m^3	Dynamic Ciscosity (μ) kg/ms	Kinematic Viscosity (ν) m^2/s
Air	1.2047	1.8205×10^{-5}	1.5111×10^{-5}
Water	998.21	1.0020×10^{-3}	1.0030×10^{-6}

3.2   Wind Speed and Reynolds Calculation

The Betz manometer measures a pressure difference between the entrance of test section and outside of the wind tunnel in millimeters of water (q). Using this measurement we can calculate the average wind speed inside the test section as well as the Reynolds number. Let's write a Bernoulli relation between outside of the wind tunnel (o) and the test section (t) as in Eq. 3.

$$P_o + \frac{1}{2}\rho_{air}V_o^2 = P_t + \frac{1}{2}\rho_{air}V_t^2 \tag{3}$$

in which V_o is zero. As a result, we can write;

$$P_o - P_t = \frac{1}{2}\rho_{air}V_t^2 \tag{4}$$

and then

$$V_t = \sqrt{\frac{P_o - P_t}{\frac{1}{2}\rho_{\text{air}}}} \tag{5}$$

The static pressure difference of a column of water can be expressed as;

$$\Delta P = \rho_{\text{water}}gh \tag{6}$$

in which g is the gravitational acceleration and h is the height of the water column. Combining equations 5 and 6;

$$V_t = \sqrt{2gh\frac{\rho_{\text{water}}}{\rho_{\text{air}}}} \tag{7}$$

Let's use $g = 9.81m/s^2$, and simplify this equation to get;

$$V_t = 4.032\sqrt{h} \tag{8}$$

in which h is in millimeters of watechange the unit of h to metersr.

Now that the average wind speed inside the test section is known, we can calculate the Reynolds number as follows;

$$Re = \frac{V_t C}{\nu_{air}} \quad \rightarrow \quad Re = 82048.930\sqrt{h} \tag{9}$$

3.3   Lift and Drag Calculation

There are two possible methods for calculating lift and drag coefficients in the present study; using the external load cell and using static pressure taps. The external balance measures the resulting drag and lift forces, which we can use to calculate C_l and C_d using

THE UNIVERSITY OF BRITISH COLUMBIA

8

the definitions of lift and drag coefficients as follows;

$$C_l = \frac{L}{\frac{1}{2}\rho_{air}V_t^2 S} \tag{10}$$

$$C_d = \frac{D}{\frac{1}{2}\rho_{air}V_t^2 S} \tag{11}$$

4   Results

In this section, the results of the experiments are presented. With the wind speed kept at 9, 18, and 27 m/s, the lift and drag forces are measured in a range of α of -8 to 32 degrees for a wing with a span of 10 AL + 1 Wooden. The results of these measurement are presented in tables 4, 5, and 6.

Table 4: Lift and drag force vs. angle of attack at 9 m/s and full span.

Angle of Attack [°]	Lift Reading	Drag Reading
-8	-0.046	0.152
-4	0.948	0.157
0	0.958	0.342
4	1.427	0.502
8	1.988	0.717
12	2.455	0.899
16	2.86	1.164
20	3.007	1.431
24	3.293	1.756
28	3.44	2.064
32	3.415	2.435

THE UNIVERSITY OF BRITISH COLUMBIA

Table 5: Lift and drag force vs. angle of attack at 18 m/s and full span.

Angle of Attack [°]	Lift Reading	Drag Reading
-8	-0.108	0.545
-4	4.628	0.586
0	9.503	0.81
4	14.417	1.235
8	18.77	1.875
12	10.485	3.828
16	11.912	4.87
20	13.634	6.036
24	14.042	7.225
28	21.448	8.471
32	18.336	9.203

Table 6: Lift and drag force vs. angle of attack at 27 m/s and full span.

Angle of Attack [°]	Lift Reading	Drag Reading
-8	0.086	1.037
-4	10.672	1.231
0	21.964	1.861
4	33.525	2.818
8	44.282	4.268
12	53.755	5.934
16	58.187	8.929
20	58.219	11.512
24	51.39	15.897

Keeping the wind velocity at 18 m/s and removing one of the aluminum blocks, we recorded the lift and drag forces in a range of α of -8 to 32 degree. These results are presented in table 7. The same data acquisition is conducted removing another aluminum block for which the results are presented in table 8.

Table 7: Lift and drag force vs. angle of attack at 18 m/s wind speed with a span of 9 AL + 1 Wooden.

Angle of Attack [°]	Lift Reading	Drag Reading
-8	0.112	0.456
-4	4.067	0.557
0	8.193	0.802
4	12.47	1.244
8	16.343	1.882
12	8.203	3.663
16	10.305	4.534
20	12.084	5.54
24	12.427	6.632
28	20.292	7.504
32	16.24	8.887

Table 8: Lift and drag force vs. angle of attack at 18 m/s wind speed with a span of 8 AL + 1 Wooden.

Angle of Attack [°]	Lift Reading	Drag Reading
-8	0.176	0.599
-4	3.574	0.687
0	6.98	0.943
4	10.827	1.417
8	14.181	1.999
12	17.105	2.605
16	9.57	4.307
20	10.957	5.27
24	10.947	6.101
28	16.225	7.206
32	14.599	8.193

5   Discussion

In the current section the forces are calibrated and used to answer the questions.

5.1   A. Drag and Lift Coefficients vs. Angle of Attack

Using Eqs. 1 and 2 we can calibrate our raw data. Then, using Eqs. 10 and 11, the lift and drag coefficients are calculated. Keep in mind that we have to calculate the lift and drag coefficients per unit span. This means that we need to divide the calibrated lift and drag by the span of the airfoil. These results are presented in tables 9, 10, 11, 12, and

THE UNIVERSITY OF BRITISH COLUMBIA

13. Fig. 8 and 9 show the lift and drag coefficients vs. angle of attack for the full span case, respectively. Three curves are present in these figures which correspond to different wind velocities. The coefficient of lift is lowest for 9 m/s case and it increases continuously with increase in angle of attack. It follows the same trend till 8 angle of attack for 18 m/s and 27 m/s cases. As we go on increasing the angle of attack from 8 to 12 for 8 m/s case, the flow separation occurs on the upper surface of the wing and it results in the decrease in the lift coefficient. The flow transition on the upper surface of the wing again results in increase in the lift coefficient after 12 angle of attack and it reaches a maximum value at 28 angle of attack. For 27 m/s case, the lift coefficient increases continuously till 18 angle of attack at which stall occurs and it starts decreasing after the stall. It can be concluded from the results that the amount of lift generated on the wing increases with increase in wind velocity. It is quite evident from the figure that the increase in the angle of attack results in the increase in the drag force on the wing. The drag coefficient is maximum for 9 m/s case for -8 to 10 degrees angle of attack. The drag coefficient curve for 18 m/s and 27 m/s case follows the almost same line for -8 to 8 degrees angle of attack. For 18 m/s case, the drag force on the wing increases significantly over the small range of angle of attack due to flow separation on the upper surface of the wing and it remains maximum for more than 12 degrees angle of attack. The drag coefficient curve follows the same trend for all three cases for more than 24 degrees angle of attack.

Fig. 10 and 11 show the lift and drag coefficients vs. angle of attack at $V = 18$ m/s. Three curves are present in these figures which correspond to different spans. The lift coefficient lines follow almost the same trend for all three cases for -8 to 5 angle of attack. It reaches to a maximum value at 7.5 degrees and starts decreasing after that for 10 and 9 AL section wings. While for 8 AL section wing, it goes on increasing and reaches a peak at 12 angle of attack. The low aspect ratio wing gives high lift and stall occurs at a higher angle of attack. The drag coefficient is plotted against the angle of attack for wing with different aspect ratios in the figure . The figure shows that the wing with low aspect ratio experiences higher amount of drag force as the low aspect ratio wing generates the more amount of induced drag. The drag coefficient curve follows the almost same trend for higher aspect ratio wings. The same trend in the coefficient of lift curves is observed for all three wing configurations for more than 16 angle of attack. Fig. 12 and 13 show drag polar for the full span wing and different velocities, and different span wings at $V = 18$ m/s, respectively.

THE UNIVERSITY OF BRITISH COLUMBIA

Table 9: Calibrated lift and drag forces per unit span vs. angle of attack for $V = 9$ m/s a span of 10 AL + 1 Wooden.

Angle of Attack [°]	Drag [N]	Lift [N]	C_d	C_l
-8	0.139996	-0.04429	0.032944	-0.010422
-4	0.144986	0.9732676	0.034119	0.229033
0	0.329616	0.9835046	0.077566	0.231442
4	0.489296	1.4636199	0.115143	0.344424
8	0.703866	2.0379156	0.165636	0.479569
12	0.885502	2.5159835	0.208379	0.592069
16	1.149972	2.930582	0.270615	0.689634
20	1.416438	3.0810659	0.333321	0.725046
24	1.740788	3.3738441	0.409648	0.793944
28	2.048172	3.524328	0.481983	0.829356
32	2.41843	3.4987355	0.569113	0.823334

Table 10: Calibrated lift and drag forces per unit span vs. angle of attack for $V = 18$ m/s a span of 10 AL + 1 Wooden.

Angle of Attack [°]	Drag [N]	Lift [N]	C_d	C_l
-8	0.53221	-0.10776	0.03131	-0.00634
-4	0.573128	4.7404836	0.033718	0.278887
0	0.79668	9.7310211	0.046869	0.572484
4	1.22083	14.7614829	0.071822	0.86843
8	1.85955	19.217649	0.109399	1.13059
12	3.808644	10.7362945	0.224066	0.631625
16	4.84856	12.1971144	0.285245	0.717566
20	6.012228	13.9599258	0.353704	0.821274
24	7.19885	14.3775954	0.423514	0.845846
28	8.442358	21.9591176	0.496671	1.291873
32	9.172894	18.7733632	0.539649	1.104452

THE UNIVERSITY OF BRITISH COLUMBIA

Table 11: Calibrated lift and drag forces per unit span vs. angle of attack for $V = 27$ m/s a span of 10 AL + 1 Wooden.

Angle of Attack [°]	Drag [N]	Lift [N]	C_d	C_l
-8	1.023226	0.090838	0.026754	0.002375
-4	1.216838	10.9277264	0.031817	0.285728
0	1.845578	22.4873468	0.048256	0.587977
4	2.800664	34.3223425	0.073229	0.897427
8	4.247764	45.3342834	0.111066	1.185357
12	5.910432	55.0317935	0.15454	1.438918
16	8.899442	59.5688319	0.232694	1.557548
20	11.477276	59.6015903	0.300097	1.558405
24	15.853506	52.610743	0.414522	1.375615

Table 12: Calibrated lift and drag forces per unit span vs. angle of attack for $V = 18$ m/s a span of 9 AL + 1 Wooden.

Angle of Attack [°]	Drag [N]	Lift [N]	C_d	C_l
-8	0.443388	0.117454	0.02863	0.007584
-4	0.544186	4.1661879	0.035138	0.269012
0	0.788696	8.3899741	0.050926	0.541744
4	1.229812	12.768339	0.079409	0.824457
8	1.866536	16.7331291	0.120523	1.080465
12	3.643974	8.4002111	0.235293	0.542405
16	4.513232	10.5520285	0.291421	0.681349
20	5.51722	12.3731908	0.356249	0.798942
24	6.607036	12.7243199	0.426619	0.821615
28	7.477292	20.7757204	0.482812	1.341497
32	8.857526	16.627688	0.571934	1.073657

THE UNIVERSITY OF BRITISH COLUMBIA

Table 13: Calibrated lift and drag forces per unit span vs. angle of attack for $V = 18$ m/s a span of 8 AL + 1 Wooden.

| Angle of Attack [°]	Drag [N]	Lift [N]	C_d	C_l
-8	0.586102	0.182971	0.041936	0.013092
-4	0.673926	3.6615038	0.04822	0.261984
0	0.929414	7.148226	0.0665	0.511463
4	1.402466	11.0863999	0.100348	0.793243
8	1.983302	14.5198897	0.141907	1.038913
12	2.58809	17.5131885	0.18518	1.253086
16	4.286686	9.799609	0.306717	0.701172
20	5.24776	11.2194809	0.375482	0.802765
24	6.077098	11.2092439	0.434822	0.802033
28	7.179888	16.6123325	0.513728	1.188629
32	8.164914	14.9477963	0.584208	1.06953
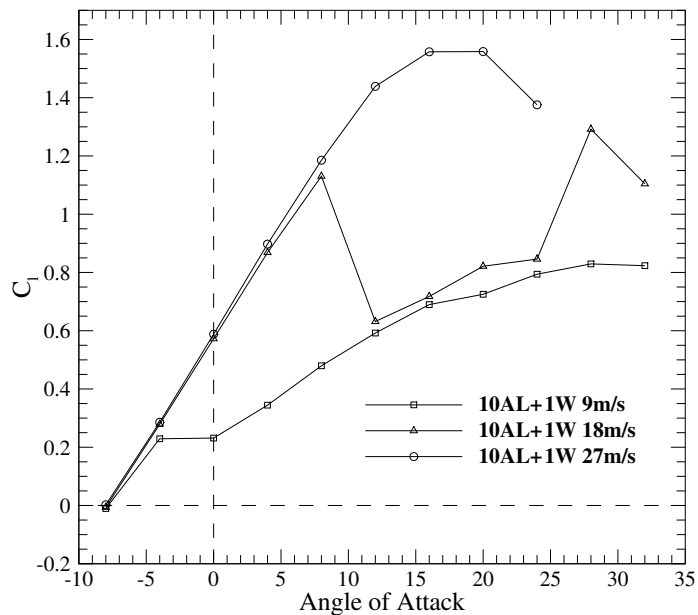
Figure 8: Lift coefficient vs. angle of attack for the full span case.
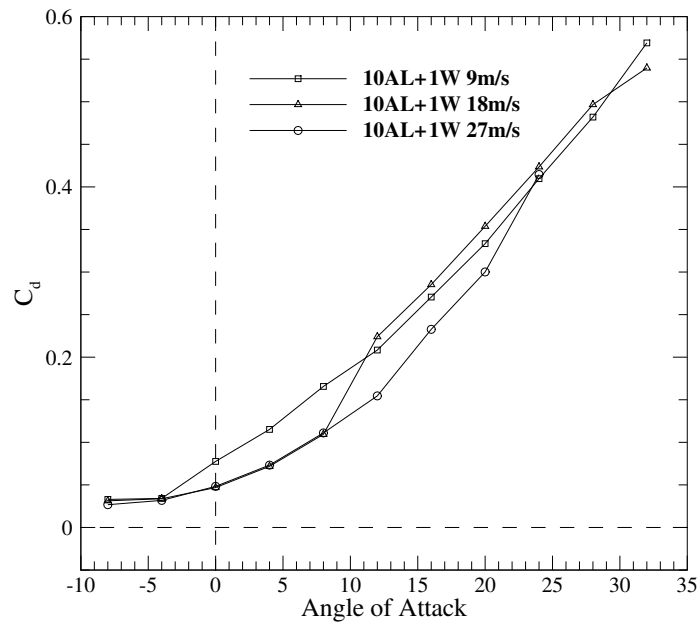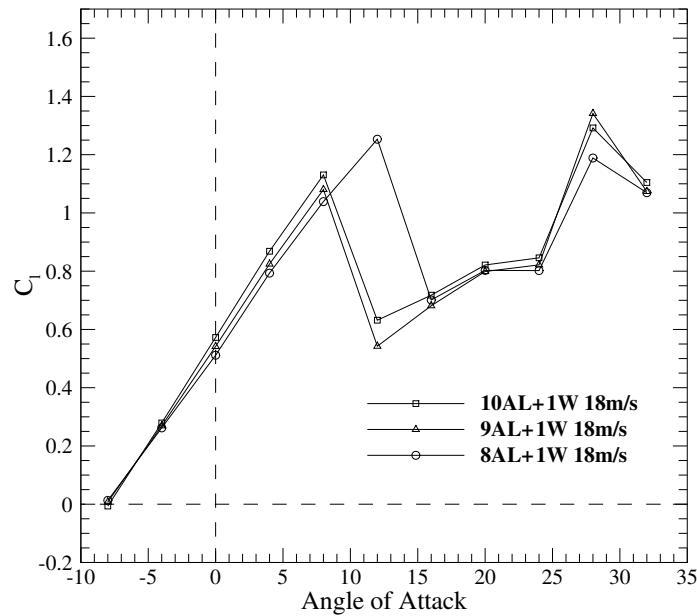
Figure 9: Lift coefficient vs. angle of attack for the full span case.


Figure 10: Lift coefficient vs. angle of attack at $V = 18$ m/s and different spans.
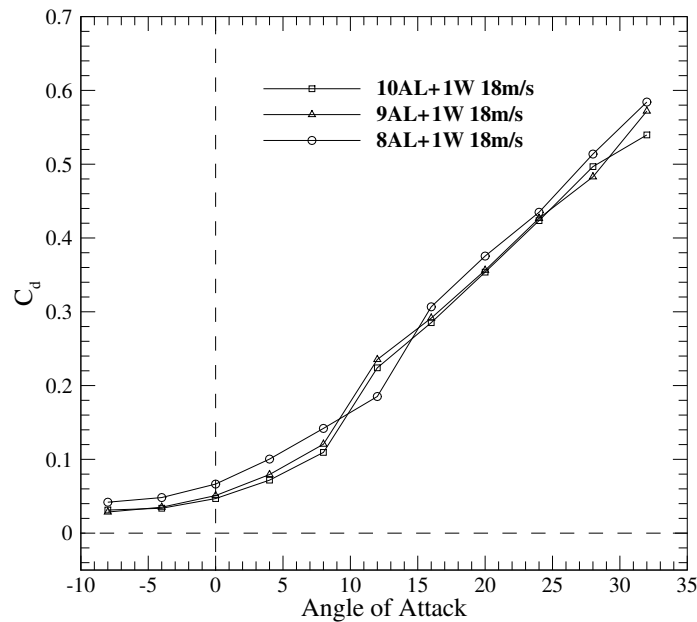
Figure 11: Lift coefficient vs. angle of attack at $V = 18$ m/s and different spans.
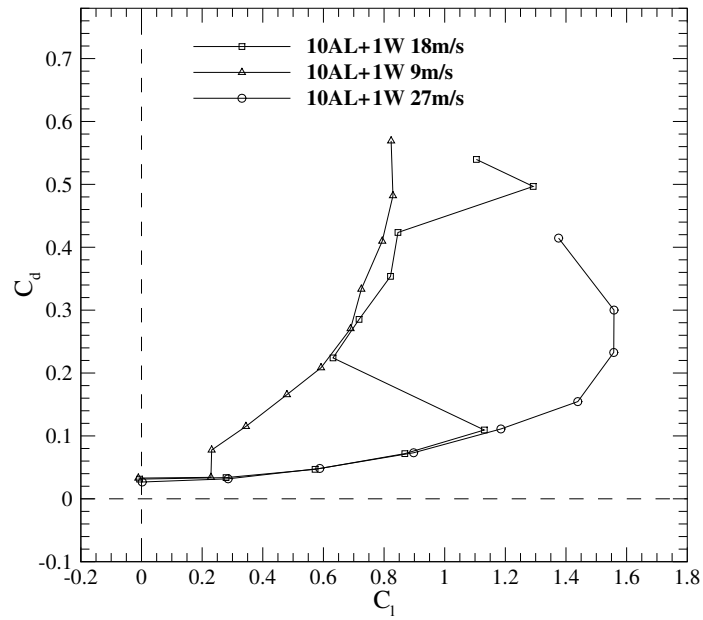
Figure 12: Drag polar for the full span wing at different wind velocities.
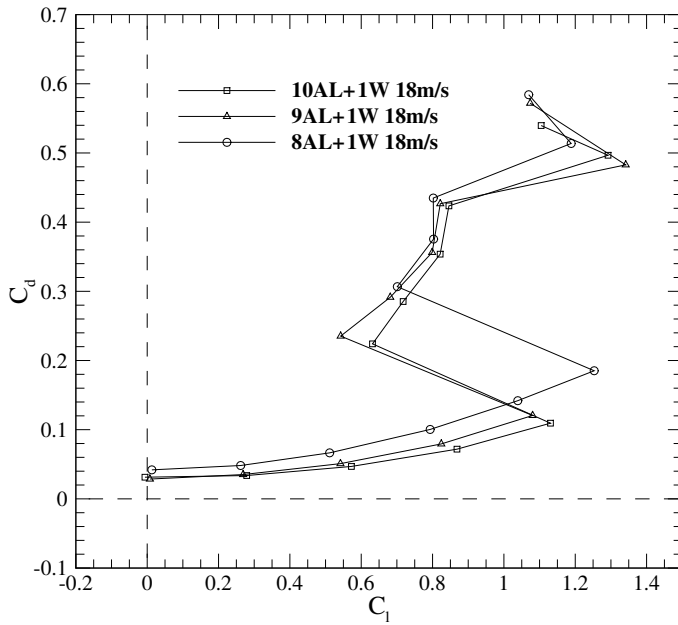
Figure 13: Drag polar at $V = 18$ m/s and different spans.

5.2   E. Uncertainty Analysis

The term uncertainty is used to refer to a "possible value that an error may have". It is necessary to make a distinction between single sample and multiple sample uncertainty analysis. The distinction hinges on whether or not a "large" or "small" number of independent data points are taken at each test point and on how the data are handled. Uncertainties for the experimentally measured lift coefficient are evaluated in this section. The methodology for estimating uncertainties follows the AIAA S-071 Standard as presented in [1] for multiple tests (sections 6.1 and 6.3). Uncertainties include various parameters such as; reading errors, measurement errors, calibration error and so on. Sources of error of the present experiment can be summarized as:

- Measurement system errors

- Noise or random errors

- Reading errors

- Calibration errors

- Errors in airfoil geometry and manufacturing which accounts for the errors in pressure tap positions as well

UBC THE UNIVERSITY OF BRITISH COLUMBIA

Consider a variable x_i which has a known uncertainty δx_i. The form of representation of this variable and its uncertainty is:

$$x_i = \overline{x}_i \pm \delta x_i \quad [P\%] \tag{12}$$

In this equation, $\overline{x}_i$ is the best estimate of x_i. Also, there is $P\%$ chance that this statement is true. Further, δx_i represents 2σ for a single sample analysis in which σ is the standard deviation of population of a possible data set.

The results R of the experiment is assumed to be calculated as a function of a number of independent parameters represented by:

$$R = R(x_1, x_2, \ldots, x_m) \tag{13}$$

The effect of the uncertainty in a single measurement on the calculated results is:

$$\delta Rx_i = \frac{\partial R}{\partial x_i} \delta x_i \tag{14}$$

$\dfrac{\partial R}{\partial x_i}$ is the sensitivity coefficient for the results R with respect to measurement x_i. When several independent variables are used in the function of R, the individual terms are combined by RSS method.

$$\delta R = \left(\sum_{i=1}^{m} \left(\frac{\partial R}{\partial x_i} \delta x_i \right)^2 \right)^{0.5} \tag{15}$$

Unlike a multiple sample experiment, in which the variable error in a set of measurements can be determined from variance, simple sample experiments require an auxiliary experiment in order to estimate the variable component of the uncertainty. This usually takes the form of a set of independent observations of the process at a representative test condition over a representative interval of time. The principal difficulty here is finding σ, the standard deviation of the population from a smaller than infinite set of observations. σ is different from the standard deviation of the set of observations made in the auxiliary experiment, but can be estimated from it. In single sample uncertainty analysis, each measurement is assigned three uncertainty value; zero, first and Nth order uncertainties.

5.2.1 Zero order uncertainty

The zero order uncertainty of a measurement is the RSS combination of all the fixed and random uncertainty components introduced by the measuring system.

5.2.2 First order uncertainty

The first order uncertainty of a measurement describes the scatter that would be expected in a set of observation using the given apparatus and instrumentation system, while the observed process is running. The first order uncertainty includes all effects of process

unsteadiness as well as the variable error effects from the measuring system. The first order uncertainty interval must be measured in an auxiliary experiment.

5.2.3   Nth order uncertainty

The Nth order uncertainty of a result is a measure of its overall uncertainty, accounting for all sources of fixed and variable errors. This is the value that should be reported as the overall uncertainty. The Nth order uncertainty is calculated as the RSS combination of the first order uncertainty and the fixed errors from every source.

Now we can calculate the uncertainty in C_l from Sec. 5.1. For this purpose the uncertainties can be summarized as follows:

- Error in lift calibration, u_c.

- Error in reading the Betz manometer, $u_{Betz} = \dfrac{0.1}{2} = 0.05$. This manometer has a precision of 0.1 and the error is half of this precision.

- Error in the data acquisition system, u_{data}. This uncertainty is equal to the maximum value of standard deviation in the readings for lift, which is 0.032.

- Error in calculating V_t, u_{V_t} which is calculated from the following equation. Be sure to change the units of h to meters.

$$u_{V_t} = h\frac{\partial}{\partial h}\left(4.032\sqrt{h}\right) = 4.032\frac{\sqrt{h}}{2} = 4.032\frac{\sqrt{0.03}}{2} = 0.3492$$

The final uncertainty can be estimated using RSS method as follows;

$$\sigma = \sqrt{\left(\frac{\partial C_l}{\partial L}u_L\right)^2 + \left(\frac{\partial C_l}{\partial V_t}u_{V_t}\right)^2}$$

$$\sigma = \sqrt{\left(\frac{2}{\rho V_t^2 C}u_L\right)^2 + \left(\frac{-4L}{\rho V_t^3 C}u_{V_t}\right)^2}$$

For $\alpha = 12$ we can calculate the error as follows. This angle of attack has the maximum lift force which accounts for the highest error possible.

$$\sigma = \sqrt{\left(\frac{2}{1.2047 \times 22.08^2 \times 0.3075}0.05\right)^2 + \left(\frac{-4 \times 59.602}{1.2047 \times 22.08^3 \times 0.3075}0.3492\right)^2} = 0.1254$$

(16)

As a result, the lift coefficient can be expressed as the following equation;

$$C_l = \overline{C_l} \pm 0.1254$$

(17)

6   Conclusion

The lift and drag coefficients over the wing are measured for a range of angle of attack and for three different wind velocities in this experiment. The results show that the lift coefficient increases significantly with an increase in wind velocity. It is evident from the results that the stall occurs at the lower angle of attack for higher wind velocity. The drag force on the wing increases with increases in the angle of attack for all three wind velocity cases. The wing with low aspect ratio stalls at a higher angle of attack and it gives higher lift at the same time it experiences the higher amount of drag force as low aspect ratio wings have more amount of induced drag. Further, the results from the experiment are different than the theoretical calculations as the theory does not consider the viscous effects of the flow and the stall phenomena.

References

[1] F. Stern, M. Muste, M.-L. Beninati, and W. E. Eichinger, "Summary of experimental uncertainty assessment methodology with example," tech. rep., IIHR Report, 1999.